African Journal of Basic & Applied Sciences 5 (4): 200-204, 2013
ISSN 2079-2034
© IDOSI Publications, 2013
DOI: 10.5829/idosi.ajbas.2013.5.4.11190

Size Dependence of H-SiNW on Band Gap along [111] Direcrion

Sana Kausar and Shirish Joshi

Department of Physics Govt. M.V.M. College Bhopal, India

Abstract: In this work band gap of hydrogen-passivated, free-standing silicon nanowires, oriented along [111] direction with rectangular cross section was studied for different area of cross section. Further the effect of cross sectional area on band structure is also analyzed by DFT using GGA approximation. it is found that the band gap of H-SiNW are dramatically altered upon changing the cross sectional area.

Key words: DFT · GGA · Nanowire

INTRODUCTION

In the last few years quantum wires, or nanowires are studied both experimentally and theoretically. Semiconductor nanowires exhibit a variety of unique material properties, including mechanical flexibility, size-dependent optical and electronic properties and solution processability. In particular, silicon nanowires (SiNWs) have been studied both theoretically [1] and experimentally [2] for a long time and they have attracted much attention due to their applications in various field, such field-effect transistors [3-5], solar cells [7,8] and energy conversion devices [9,10], nanosensors [3,6]. While developing these applications, it is important to control the electronic properties of nanowires (NWs), which strongly depend on the diameter as well as the crystallographic orientation [11], cross sectional shape and optimized structure of the NWs [12]. There are several ways due to which band structure of SiNWs can changed, for example, by changing cross sectional area, cross sectional geometry, orientation, surface morphology, dangling bond passivation and doping [1,2]. Reduced dimensionality systems are characterized by a large surface-to-bulk ratio and offer the possibility of doping through the external adsorption of molecules [13] rather than the incorporation of substitutional impurities [14]. Álvaro Miranda [15] has studied NH_3 molecular doping of silicon nanowires grown along the [112], [110], [001] and [111] orientations. Sercel [23-25] studied cylindrical GaAs/A $_{l0.3}$Ga$_{0.7}$As nanowires with infinite and finite barriers by using a four-band model using axial approximation. They have studied 1 nm radius nanowire in their calculations. More recent calculations for free-standing zinc-blende nanowires are less common. There have been calculations of nanowire band structures using the empirical tight-binding method.B. Lassen [27] has studied Electronic structure of free-standing InP and InAs nanowires. The nanowires are now mostly of the free-standing type; typical dimensions are tens of nanometers in lateral size and microns in length, although nanowires as small as 3 nm in diameter have been reported [16,17]. Not only cubic but wurtzite structure nanowires have been synthesized. They can be assumed to have low defect concentrations and close to bulk structure, few research studies have carried out on strained nanowires [18], a number of studies have already been made. polarized photoluminescence [19,20] and Raman scattering have been experimentally studied [21]. There were early calculations of the band structures of embedded nanowires using the *k_p* method. In 1989, Citrin and Chang [22] applied the six-band Luttinger-Kohn *k_p* to rectangular GaAs/Al0.2Ga0.8As nanowires, they observed that crossing behavior of the first two valence states in a square quantum wire becomes anti-crossing in a rectangular quantum [26,28] There are also a few ab initio calculations now reported for InP nanowires [29,30] though only for the bandgap and not for the whole band structure. In this article we extend our earlier study in which we have studied the size dependent of band of silicon nanowire of triangular cross section along [111] direction by implementing density functional theory using GGA,in this study size dependent of band of silicon nanowire of rectangular cross section along [111] direction by implementing density functional theory using GGA.

Corresponding Author: Sana Kausar, Department of Physics Govt. M.V.M. College Bhopal, India.

Table 1:

Si	H	Lattice parameters(A	Cell Angles	Cross sectional area (nm^2)	Band Gap (eV)
18	22	a = 20.122136	alpha = 90.079268		
		b = 19.944290	beta = 90.198734 gamma = 90.198028		
		c = 9.513158		.266	3.229
32	30	a = 30.454426	alpha = 90.000000		
		b = 30.499196	beta = 89.836100 gamma = 89.999999	.388	2.380
		c = 9.621926			
50	38	a = 27.037097	alpha = 90.000000		
		b = 30.991761	beta = 89.750330 gamma = 90.000000	.906	2.031
		c = 9.552908			

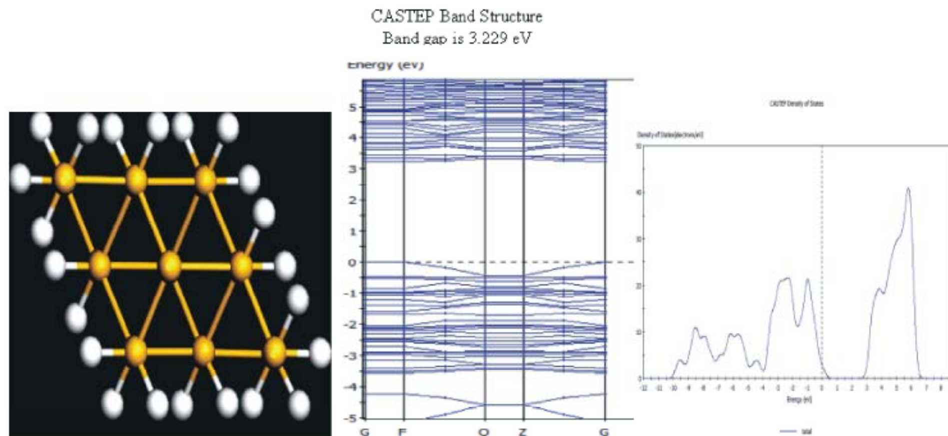

Fig. 1:

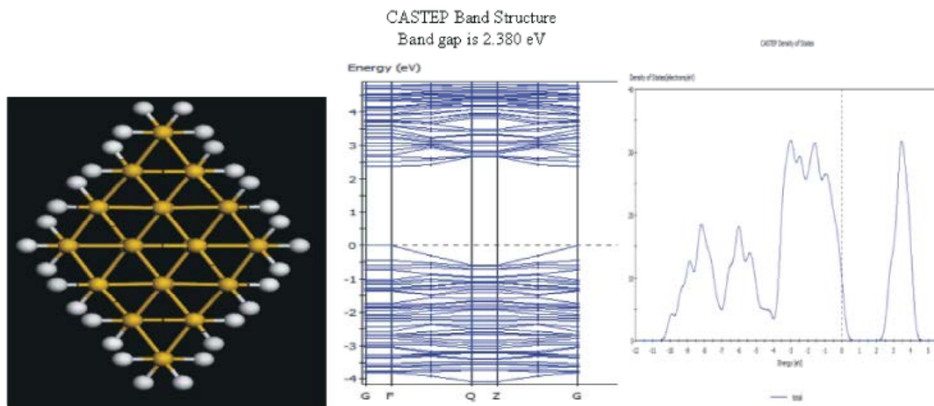

Fig. 2:

Size Dependence of the Band Gap of SiNWs Along [111] Direction: SiNWs which have rectangular cross section was chosen with different cross sectional area and the electronic band structure of these SiNWs was studied by using DFT calculation. In this study The relation between size and electronic band structure of the SiNWs observed in detail. Silicon nanowire as a prototype was taken and grown along [111] direction. The ideal nanowire is cut initially from bulk Si crystal and, subsequently, the lattice constant *co* and all the atomic positions are fully optimized. Upon relaxation, the structure of the ideal bare nanowire reconstructed. Furthermore, to allow possible reconstructions involving two unit cells, structure optimization of an ideal nanowire was carried out. In the later optimization, the energy per Si atom and the atomic structure did not change from the single cell optimization. Table 1 lists the studied cases with the atomic numbers within them, the area of the cross section and band gap. The cross section of the nanowires are rectangular along [111] SiNWs as displayed in Fig.1, Fig.2, Fig.3.

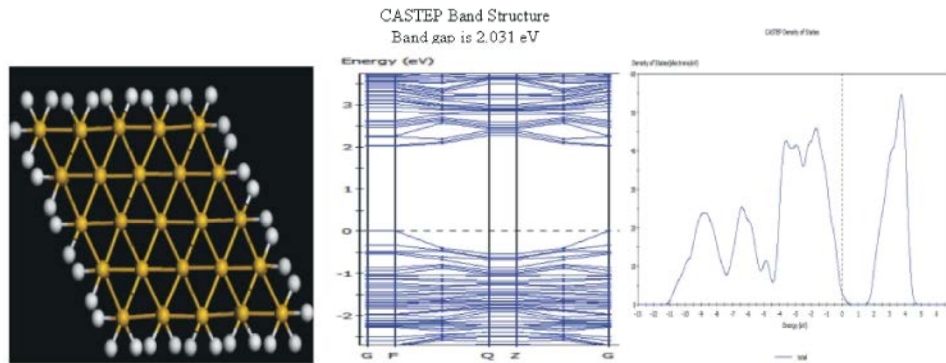

Fig. 3:

The shape of the cross section was fixed and their size was increased gradually. The lattice constants along the chain axes were optimized, involving variations within 3.5%. Senger and coauthors [38] built the silicon chains as linear or zigzag chains with varying bond angle. In contrast, our focus is on the relationship between the area of cross section and band gap. The Top (upper) View of silicon nanowire is shown in along <111> direction. Yellow spheres stand for silicon atoms and white spheres for hydrogen. Hydrogen termination is used to eliminate the defect states within the band gap so that the band structure of the chain should briefly feature the characteristics of silicon. Between two neighboring chains there is a vacuum layer thicker than 4 Å for eliminating the inter-layer interaction. The structures of hydrogen-terminated silicon chains were modeled in supercells involving two primitive unit cells. We have performed first-principles plane wave calculations [31,32] within DFT [33] using ultrasoft pseudopotentials [32,34].The exchange correlation potential has been approximated by generalized gradient approximation GGA using Perdew Burke Ernzerhof exchange correlation functional [35] both for spin-polarized and spin-unpolarized cases. For partial occupancies, we use the Methfessel-Paxton smearing method [36] The adopted smearing width is 0.1 eV for the atomic relaxation and 0.05 for the accurate band structure analysis and density of states calculations here total energy / atom convergence tolerance is 0.1000E-05 eV. All structures have been treated within a super cell geometry using the periodic boundary conditions. The lattice constants of the tetragonal super cell in the x-y plane are taken as asc=bsc=26 Å and csc=*9.406* Å along the z axis. For the double unit cell calculations, the lattice constant is taken as csc=2co to prevent the interactions between the nearest neighbor impurity atoms located in adjacent cells. In the self consistent potential and total energy calculations, the Brillouin zone of SiNW is sampled in the k space within the Monkhorst-Pack scheme [37] by 1x1x40 mesh points as determined by the convergence tests. A plane wave basis set with kinetic energy 230 eV has been used. All atomic positions and lattice parameters are optimized by using the BFGS where total energy and atomic forces are minimized. The convergence or energy is chosen as 10^{-4} eV between two ionic steps and the maximum force allowed on each atom is 0.3000E-01eV/A. The band structures around the Fermi energy levels are displayed in Fig.1,Fig.2 and Fig.3 for [111], rectangular cross sectional nanowire. Note that for a SiNW with a larger diameter, the conduction band minimum increases differently at different K points. Upon passivation with H and subsequent optimization, most of the peak positions coincide with those of the ideal SiNW.

Yellow sphere represents the silicon atom and white spheres represent hydrogen atoms. right panel represents the energy band diagrams for the optimized hydrogenated silicon nanowires along [111] direction. The zero of energy is taken at the Fermi level

CONCLUSION

Our results show that area of cross section is important factors for determining band gap. Some of the parameters that characterize the electronic band structures are listed in TABLE-1 It has been found that the band gap of the SiNWs decreases as the diameter increases. A quantity relation, that the band gap is proportional to the reciprocal of the wire diameter was revealed, which directly supports the quantum effect in experiments as well as in theory. The gap width varied from 3.229eV at. 266nm^2 to 2.031eV at about. 906nm^2. The size dependence of the band gap revealed here is evidence for quantum confinement. As the periodicity was only along the wire

axis, the movement of electrons was confined in the plane perpendicular with the wire axis. The band structure was folded, so that the energy bands near the Fermi energy level were modified seriously when the diameter of the SiNW was small. On the other hand, hydrogen termination makes the energy bands split deep in the valence bands or higher in the conduction bands. It is another but not the main reason that the band gap of the SiNWs is broadened. When the cross sectional area of the SiNW is large enough that time SiNWs will show the characteristics of the bulk silicon. In our calculations, the gap width is decreasing and converges with that of the crystalline silicon on increasing the cross sectional area.

REFERENCES

1. Rurali R. Colloquium, 2010. structural, electronic and transport properties of silicon nanowires. Rev Mod Phys., 82: 427.
2. Schmidt, V., J.V. Wittemann and U. Gösele, 2010. Growth, thermodynamics and electrical properties of silicon nanowires. Chem Rev. 110: 361. doi: 10.1021/cr900141g.
3. Cui, Y., Q. Wei, H. Park and C.M. Lieber, 2001. Nanowire nanosensors for highly sensitive and selective detection of biological and chemical species. Science, 293: 1289.
4. Jang, M., Y. Park, M. Jun, Y. Hyun, S.J. Choi and T. Zyung, 2010. The characteristics of Seebeck coefficient in silicon nanowires manufactured by CMOS compatible process. Nanoscale Res Lett., 5: 1654.
5. Moraru, D., A. Udhiarto, M. Anwar, R. Nowak, R. Jablonski, E. Hamid, J.C. Tarido, T. Mizuno and M. Tabe, 2011. Atom devices based on single dopants in silicon nanostructures. Nanoscale Res Lett., 6: 479.
6. Stern, E., J.F. Klemic, D.A. Routenberg, P.N. Wyrembak, D.B. Turner-Evans, A.D. Hamilton, D.A. LaVan, T.M. Fahmy and M.A. Reed, 2007. Label-free immunodetection with CMOS-compatible semiconducting nanowires. Nature., 445: 519.
7. Tian, B., X. Zheng, T.J. Kempa, Y. Fang, N. Yu, G. Yu, J. Huang and C.M. Lieber, 2007. Coaxial silicon nanowires as solar cells and nanoelectronic power sources. Nature. 449:885. doi: 10.1038/nature06181.
8. Ossicini, S., M. Amato, R. Guerra, M. Palummo and O. Pulci, 2010. Silicon and germanium nanostructures for photovoltaic applications: ab-initio results. Nanoscale Res Lett., 5: 1637.
9. Hochbaum, A.I., R. Chen, R. Diaz-Delgado, W. Liang, E.C. Garnett, M. Najarian, A. Majumdar and P. Yang, 2008. Enhanced thermoelectric performance of rough silicon nanowires. Nature, 451: 163.
10. Boukai, A.I., Y. Bunimovich, J. Tahir-Kheli, J.K. Yu, W.A. Goddard-III and J.R. Heath, 2008. Silicon nanowires as efficient thermoelectric materials. Nature, 451: 168.
11. Holmes, J.D., K.P. Johnston, R.C. Doty and B.A. Korgel, 2000. Control of thickness and orientation of solution-grown silicon nanowires. Science, 287: 1471.
12. Mozos, J.L., E. Machado, E. Hernandez and P. Ordejon, 2005. Nanotubes and nanowires: the effect of impurities and defects on their electronic properties. Int. J. Nanotechnol., 2: 114.
13. Schedin, F., A.K. Geim, S.V. Morozov, E.W. Hill, P. Blake, M.I. Katsnelson and K.S. Nonoselov, 2007. Detection of individual gas molecules adsorbed on graphene. Nature Mater, 6: 652.
14. Wehling, T.O., K.S. Novoselov, S.V. Morozov, E.E. Vdovin, M.I. Katsnelson, A.K. Geim and A.I. Lichtenstein, 2008. Molecular doping of graphene. Nano Lett., 8: 173.
15. Álvaro Miranda, Xavier Cartoixà, Enric Canadell and Riccardo Rurali, 2012. Nanoscale Res Lett., 7(1): 308.
16. Morales, A.M. and C.M. Lieber, 1998. A laser ablation method for the synthesis of crystalline semiconductor nanowires. Science, 279(5348): 208.
17. Duan, X. and C.M. Lieber, 2000. General synthesis of compound semiconductor nanowires. Adv. Mater., 12(4): 298.
18. Seo, H.W., S.Y. Bae, J. Park, H. Yang, K.S. Park and S. Kim 2002. Strained gallium nitride nanowires. J. Chem. Phys., 116(21): 9492.
19. Wang, Y., L. Zhang, C. Liang, G. Wang and X. Peng, 2002. Catalytic growth and photoluminescence properties of semiconductor single-crystal ZnS nanowires. Chem. Phys. Lett., 317(3-4): 314.
20. Gudiksen, M.S., J. Wang and C.M. Lieber, Size-dependent photoluminescence from single indium phosphide nanowires. J. Phys.
21. Gupta, R., Q. Xiong, C.K. Adu, U.J. Kim and P.C. Eklund, 2003. Laserinduced fano resonance scattering in silicon nanowires. Nano Lett., 3(5): 627.
22. Citrin, D.S. and Y.C. Chang, 1989. Valence-subband structures of GaAs/ AlxGa1-xAs quantum wires: The effect of split-off bands. Phys. Rev. B., 40(8): 5507.

23. Sercel, P.C. and K.J. Vahala, 1990. Analytical technique for determining the polarization dependence of optical matrix elements in quantum wires with band-coupling effects. Appl. Phys. Lett., 57(6): 545.
24. Sercel, P.C. and K.J. Vahala, 1990. Analytical technique for determining quantum-wire and quantum-dot band structure in the multiband envelope-function representation. Phys. Rev. B., 42(6): 3690.
25. Sercel, P.C. and K.J. Vahala, 1991. Polarization dependence of optical absorption and emission in quantum wires. Phys. Rev. B., 44(11): 5681.
26. Persson, M.P. and H.Q. Xu, Electronic structure of nanometerscale.
27. Lassen, B., M. Willatzen, R. Melnik and L.C. Lew Yan Voon, 2006. Materials Research Society, 21(11).
28. Persson, M.P. and H.Q. Xu, 2004. Electronic structure of [100]-oriented freestanding semiconductor nanowires. Nano Lett., 4(12): 2409.
29. Li, J. and L.W. Wang, 2005. Band-structure-corrected local density approximation study of semiconductor quantum dots and wires. Phys. Rev. B., 72(12): 125-325.
30. Schmidt, T.M., R.H. Miwa, P. Venezuela and A. Fazzio, 2005. Stability and electronic confinement of free-standing inp nanowires: *Ab initio* calculations. Phys. Rev. B., 72(16): 193-404.
31. Payne, M.C., M.P. Teter, D.C. Allen, T.A. Arias and J.D. Joannopoulos, 1992. Rev. Mod. Phys., 64: 1045.
32. Kresse, G. and J. Hafner, 1996. Numerical computations have been carried out using VASP software., Phys. Rev. B 47, R558, 1993. G. Kresse and J. Furthmuller, ibid., 54: 11169.
33. Kohn, W. and L.J. Sham, 1965. Phys. Rev. 140, A1133.
34. Hohenberg, P. and W. Kohn, 1964. Phys. Rev., 136: B864.
35. Vanderbilt, D., 1990. Phys. Rev. B 41, R7892.
36. Perdew, J.P., J.A. Chevary, S.H. Vosko, K.A. Jackson, M.R. Pederson, D.J. Singh and C. Fiolhais, 1992. Phys. Rev. B., 46: 6671.
37. Methfessel, M. and A.T. Paxton, 1989. Phys. Rev. B., 40: 3616.
38. Monkhorst, H.J. and J.D. Pack, 1976. Phys. Rev B., 13: 5188.
39. Senger, R.T., S. Tongay, E. Durgun and S. Ciraci, 2005. Phys. Rev B., 72: 075419.